Failure Modes of Underground MV Cables: Electrical and Thermal Modelling.

Peter A Wallace*, Mohamed Alsharif, Donald M Hepburn and Chengke Zhou
Glasgow Caledonian University
*Corresponding author: Department of Energy Systems Engineering, Glasgow Caledonian University, Glasgow G4 0BA, UK, pwa@gcal.ac.uk

Abstract: Two simulations of the performance of a Paper Insulated Lead Covered (PILC) medium voltage (MV) underground cable are presented. The first presents the thermal response of a cable, over seven days, to a realistic load with a diurnal variation. The second concentrates on the variation of the electric field stress within the cable over a single a.c. cycle. The effects of a void defect within the insulation are presented. Finally the electric stress within the insulation of one conductor is resolved into components normal and tangential to the lie of the insulating paper tape.

Keywords: MV cables, heat transfer, electrostatics

1. Introduction

Medium Voltage (MV) electricity distribution systems often rely on underground cables carrying some hundreds of amperes at voltages between 11 and 33 kV. In the UK, many of these cables have been in service for 50 years and are now operating beyond their design lifetime. Sudden failure can have serious, and expensive, consequences for the utility provider and its customers. The rate at which the cables can be replaced is limited by the cost and indeed the disruption caused by the works. It would therefore be very valuable to have a reliable on-line condition monitoring technique to apply to this problem so that repair and replacement work can be prioritized most effectively. Some of the present authors have been active in this area [1,2]. However, in order to extract the maximum quantity of information from the measured data it is necessary to understand the failure modes of the cables.

A significant cause of underground cable failures is the breakdown of the electrical insulation between the conductors due to the occurrence of internal partial discharge (PD) activity. PD in insulation material is usually caused by inhomogeneous electrical fields around voids, bubbles or defects. A gas-filled void has a lower electric permittivity and breakdown strength than that of the original insulation material. PD is initiated when the electric field across the cavity exceeds the gas breakdown strength and an initiating electron is present.

One of the most important issues is the operating temperature and indeed the thermal history of the cable. There are several factors which will determine the thermal behaviour of a given cable installation. These include the assumed ampacity, the cable construction and circumstances of installation, the thermal properties of the surrounding soil and the ambient temperature. The work presented in this paper involves the use of COMSOL multiphysics to develop an integrated electrical, thermal and mechanical model of a buried multiphase cable that simulates the behaviour occasioned by a varying load. Of particular interest will be the variation in size, shape, temperature and pressure of gas filled voids within the insulation.

2. Use of COMSOL Multiphysics

Two very different timescales are of interest in this problem. The PD events occur within the context of the 20 ms alternating current cycle. The thermal effects, in contrast, manifest themselves over hours or days and this work follows the practice, common in the field, of simulating at least a week (168 hours) of activity. Two separate models have therefore been created. One will deal with the thermal (and eventually mechanical) dynamics of the system while the second will simulate the instantaneous electrostatic phenomena that occur against the background of the effectively static temperature (and strain) distributions calculated within the first model. At present, only the electrostatic and thermal parts of the simulation have been implemented.

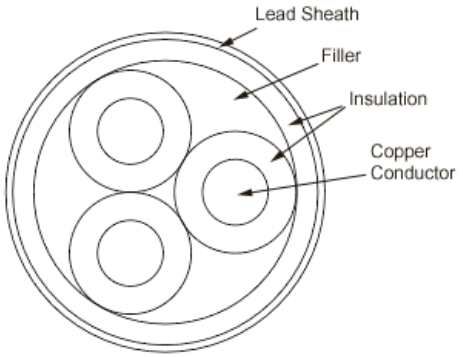

Figure 1. Geometry of three phase Paper Insulated Lead Covered (PILC) cable. The insulation comprises wound, oil impregnated paper tape.

Various configurations of legacy cable are of interest but this paper concentrates on the three phase Paper Insulated Lead Covered (PILC) cable type shown schematically in Figure 1. In this type of cable the three conductors are wrapped in oil impregnated paper tape. The three insulated cores are bundled together under another belt of paper insulation and the whole ensemble is covered in a lead sheath which provides a single earth screen for all three phases.

2.1 Thermal Model

The COMSOL Conduction application mode solves the following PDE :

$$\rho C_p \frac{\partial T}{\partial t} + \nabla \cdot (k \nabla T) = Q \qquad (1)$$

where ρ is the density, C_p is the specific heat capacity, k the thermal conductivity and Q is the heat source term. The cable is modelled as being buried in a 0.6 m square, sand filled, trench. The cable centre is at a depth of 0.3 m and the surface of the trench is flush with the surrounding soil surface. Equation (1) is solved on a 2 dimensional domain which comprises the cable cross-section of Figure 1 set in a 6 m diameter semicircle of surrounding soil and trench-fill. The boundary of the domain of solution comprises (a) the soil surface, (b) the 3 m distant semicircular boundary within the native soil. Both parts of the boundary are set to 288 K (15 °C) following [3]. The thermal conductivities of the soil and sand are set to 0.833 $Wm^{-1}K^{-1}$ and 0.2 $Wm^{-1}K^{-1}$ respectively [3]. The thermal conductivity of the cable insulation and filler is assumed to be 0.16 $Wm^{-1}K^{-1}$.

At present, the heating terms are calculated using the prescription of IEC 60287 [4] which provides methods for the calculation of the ampacity of cables according to their configuration and installation. The two heat source terms considered are the Ohmic loss due to the current flowing in the conductor, Q_c, and the loss in the sheath due to the induction of eddy currents, Q_s. In both cases the heat source terms are calculated by dividing the total loss in the conductor (sheath) by the cross-sectional area of the conductor (sheath). Hence the term Q_c is given by

$$Q_c = \frac{I^2 R}{A_c} \qquad (2)$$

where R is the a.c. resistance of the conductor per unit length

$$R = R'(1 + y_s + y_p) \qquad (3)$$

and $R'(T)$ is the d.c. resistance per unit length. y_s and y_p are the skin and proximity effects respectively and are calculated according to IEC 60287. Q_s, the sheath loss is defined in terms of Q_c.

$$Q_s = \lambda \frac{Q_c}{A_s} \qquad (4)$$

where the loss factor λ is calculated in terms of R, R_s (the sheath resistance/m) and the cable geometry according to the prescription of IEC 60287. The transfer of heat to the surroundings is governed by the geometry and material properties of the conductor, insulation, screening, sheathing and trench fill material as well as the ambient conditions. The thermal and electrical systems are coupled via the temperature dependence of the resistivities of the

conductor and sheath materials. The input data to the model is provided in the form of time series describing the variations in load over a seven day cycle and the output takes the form of the thermal response of the cable for given installation and ambient conditions.

2.1.1 Response to a static load

When this system is subject to a load step of 100 amperes the response is as shown in Figure 2. The upper curve represents the temperature at a point within the conductor while the lower (cooler) curve represents the temperature of the surface of the sheath. The response curves exhibit a fast and a slow component. The fast component may be interpreted as the relatively rapid heating of the cable itself while the slower component describes the effect of the gradual heating of the trench fill material surrounding the cable. Even after two weeks the system has not quite reached thermal equilibrium, although a steady temperature difference of approximately 10 K has been established between the conductor cores and the sheath.

2.1.2 Response to diurnal variation in load

The simulation was re-run using as input data a time series representing a real load measured over a one week period and reported in [1].

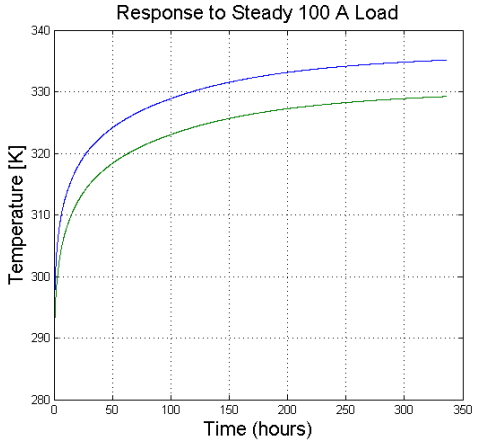

Figure 2. Thermal response of the installed cable to a load step input impressed at time t = 0 assuming an ambient temperature of 288 K. The upper curve relates to the temperature of a conductor core, the lower curve refers to the temperture of the surface of the sheath.

The diurnal variation in load produces a corresponding variation in cable operating tempeature of 15-18 K as shown in figure 3. As before the heating load was impressed into a pre-existing state of thermal equilibrium where the ambient temperature was a uniform 288 K. By the end of the week the cable operating temperature had climbed to a maximum value of 326 K (53 °C). In contrast to the static load case the temperature difference between cable centre and sheath varies between 2 and 10 K depending on the load conditions.

2.2 Electrostatic Model

COMSOL's electrostatic application mode solves Poisson's equation ,

$$-\nabla\cdot\left(\varepsilon_0\varepsilon_r\nabla V\right)=\rho \qquad (5)$$

and obtains the electric field **E** from the gradient of the potential

$$\mathbf{E}=-\nabla V \qquad (6)$$

The PDE (5) is solved subject to the following boundary conditions :

Sheath : $V = 0$

Conductors : $V(t) = V_0\cos(\omega t + 2n\pi/3)$

$n =$ 0,1,2

on the 2 dimensional domain represented by the cable cross-section. V_0 is set at 11 kV, ε_r is taken as 6 for the insulation and filler and space charge effects are presently neglected.

Figure 4 shows the field distribution in an ideal, flawless, cable. The presence of a void within the insulation will result in a local increase in the electric stress. To demonstrate this effect a 0.5 mm diameter void was introduced into the insulation belt of the right hand conductor. The void is placed on the horizontal symmetry axis of the cable, within the insulation belt, just to the right of the cable centre. Figure 5 shows the horizontal component of the electric field, $\mathbf{E}_x$, plotted along the horizontal symmetry axis. The curve represents $\mathbf{E}_x$ at the point during the a.c. cycle when the right hand conductor is at maximum (negative) potential. This axis runs between the two left hand conductors, through the void and then through the right hand conductor. The sharp increase in electric stress occasioned by the presence of the void is clearly

seen in the figure (Fig. 5) at $x = 0.003$ m

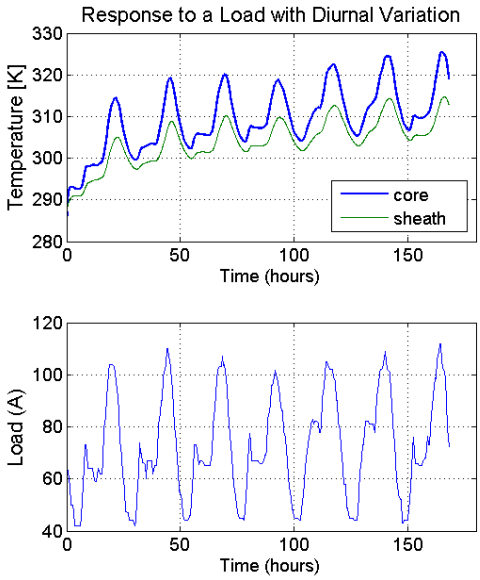

Figure 3. Upper portion of figure describes the thermal response of the cable to a diurnal variation in load over a period of seven days. The two curves correspond to a conductor core and to the sheath. Lower portion of figure displays the input load data.

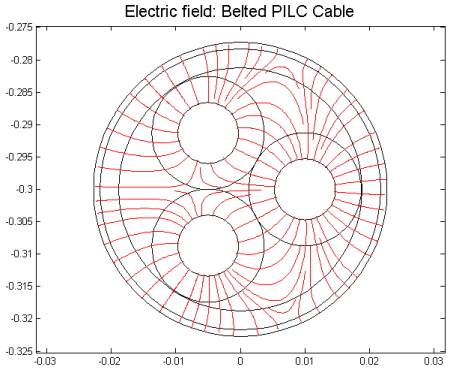

Figure 4. The electric field distribution within the cable at the point in the a.c. cycle where the potential of the right hand conductor is at its maximum value.

2.2.2 Interaction of Electric Field Stress and Cable Construction.

Figure 4 shows the electric field distribution within the cable at the point in the a.c. cycle where the potential of the right hand conductor is at its maximum value. The electric field distribution is complicated and continuously varying. In most locations, at a given point in time, within the cable the electric field is more or

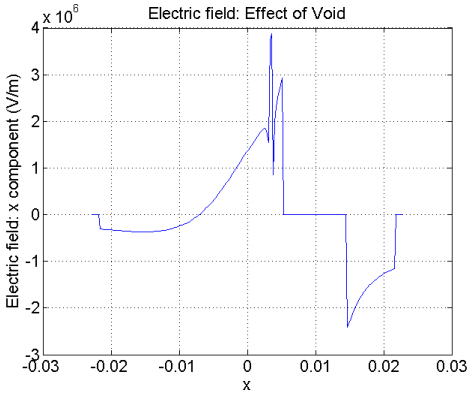

Figure 5. The horizontal component of the electric field plotted along the horizontal symmetry axis of the cable at the point when the conductor located at x = 0.01 m is at maximum (negative) potential. Note the presence of the void at a position of approximately x = 0.003 m

less normal to the direction in which the paper insulation is laid, which is to say the direction in which the strength of the insulation is greatest. However there are locations where the electric field has a significant component tangential to the paper direction.

In order to study this phenomenon the voltage solution calculated within Comsol was exported to Matlab on a regular grid. The x and y components of the electric field were calculated by differentiation and the following transformation applied to the components of E in order to obtain the tangential and radial components of the field,

$$E_T = E_X \cos\alpha + E_Y \sin\alpha$$
$$E_R = -E_X \sin\alpha + E_Y \cos\alpha \qquad (7)$$

where $\alpha = \theta - \pi/2$ and θ is the polar angle with respect to the centre of the conductor in question. Finally, since the designation of tangential and radial directions is only meaningful for one insulator belt, namely the one centred on the origin of the coordinate system, a mask is applied to the transformed field components to isolate the insulator belt. The results of such a procedure are shown in figure 6 for the insulation belt of the right hand conductor of figure 4.

It can be seen that the field in the insulation belt is affected by the superposed fields of the neighbouring conductors. These give rise to distinct regions within the insulator where there exists a considerable field component parallel to the lie of the paper insulating tape.

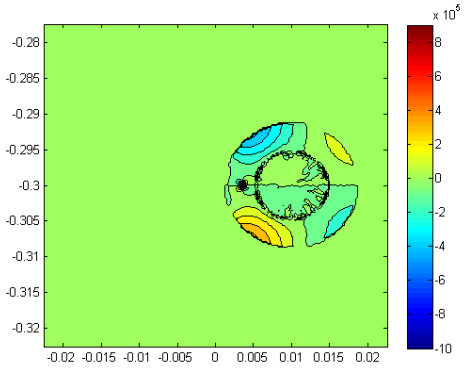

Figure 6. Contour plot of the tangential component of the electric field stress in the insulation belt of the right hand conductor of figure 4.

4. Discussion

Two models of three phase PILC distribution cables have been presented. The first seeks to represent the long term thermal response of a buried cable to an impressed electrical load. The second model examines the interaction of the cable structure, and defects therein, with the instantaneous value of the electrical stress.

Future work will add thermally induced mechanical stress to the long term model and then seek to use the resultant hot, deformed structure as the domain on which the electrostatic model will be solved in order to gain insight into the observed time structure of PD activity in such cables.

5. References

1. D M Hepburn, C Zhou, X Song, G Zhang and M Michel, 2008, "Analysis of On-line Power Cable Signals", *Int. Conf. Condition Monitoring and Diagnosis*, Beijing, China, p.1175-1178 (2008)
2. C Zhou, D M Hepburn, M Michel, X Song and G Zhang, 2008, "Partial Discharge Monitoring in medium Voltage Cables", *Int. Conf. Condition Monitoring and Diagnosis*, Beijing, China, p.1021-1024 (2008)
3. IEC 60287-3-1:1995, *Electric cables – calculation of current rating - Part 3: sections on operating conditions*
4. BS IEC 60287-1-1:2006, *Electric cables – calculation of current rating - Part 1-1: Current rating equations (100% loss factor) and calculation of losses – General.*